Hindawi
Complexity
Volume 2019, Article ID 6101083, 7 pages
https://doi.org/10.1155/2019/6101083

Research Article

Origin of Non-Gaussian Velocity Distribution Found in Freestanding Graphene Membranes

Yue Kai,[1] Wenlong Xu,[1] Bailin Zheng,[1] Nan Yang,[1] Kai Zhang,[1] and P. M. Thibado[2]

[1]*School of Aerospace Engineering and Applied Mechanics, Tongji University, Shanghai 200092, China*
[2]*Department of Physics, University of Arkansas, Fayetteville, AR 72701, USA*

Correspondence should be addressed to Bailin Zheng; blzheng@tongji.edu.cn

Received 26 January 2019; Accepted 20 February 2019; Published 13 March 2019

Academic Editor: Dimitri Volchenkov

In this study, an analytic derivation is made for the truncated Cauchy-Lorentz velocity distribution experimentally observed in freestanding graphene membranes. Three methods are used and discussed, including the Fokker-Planck-Kolmogorov equation, the maximum nonsymmetric entropy principle, and the Bayesian inference. From these results, a physical mechanism is provided for the non-Gaussian velocity distribution in terms of carbon atom arrangement in freestanding graphene. Moreover, a new theoretical foundation is proposed for future studies of the anomalous dynamics of carbon atoms in graphene membranes.

1. Introduction

The random motion of pollen particles in a fluid was first observed by Robert Brown [1, 2]. Later, Albert Einstein established the molecular theory of Brownian motion through a combination of fluid mechanics and diffusion theory [3]. He proved that Brownian particles follow a Gaussian distribution and discovered the now famous formula for the mean-squared displacement ($\langle x^2 \rangle \propto t$). In fact, Albert Einstein was the first person to describe this natural phenomenon using a stochastic process. In 1908, Jean Baptiste Perrin experimentally proved Albert Einstein's results [4]. Following Einstein, Paul Langevin proposed using a kinematic approach [5]

$$m\ddot{x} = -\lambda\dot{x} + \xi(t), \tag{1}$$

where $\xi(t)$ is a Gaussian variable. Langevin's equation is regarded as the first time a stochastic differential equation was used to describe a random process. However, scientists have found many random processes that do not follow the classical theory of Brownian motion. For this reason, the traditional Langevin equation has been generalized (see [6] and references therein):

$$m\dot{v} = f(v,t) + g(v,t)\,\xi(t), \tag{2}$$

where the $f(v,t)$ is the generalized force and $g(v,t)$ is the strength of the random force.

One nonclassical example was found by Paul Lévy, where a particle's trajectory may involve many different scales [7]. The particle will follow the classical theory of Brownian motion in a small neighborhood but then jump suddenly over a large distance to a new neighborhood, where it reverts to the classical movement. This phenomenon is known as a Lévy walk, with the mean-squared displacement given by

$$\left\langle x^2 \right\rangle \propto t^{\delta}, \tag{3}$$

where δ is a constant. With this notation, when $\delta = 1$ the particle undergoes normal Brownian motion; if $\delta = 2$, the particle is ballistic. For the condition of turbulent motion in an open system, the parameter can be $\delta = 3$ [8]. A maximum entropy approach under a variety of constraints of deriving Lévy style distributions can be seen in [9]. Recently, it was experimentally found that the jittery out-of-plane motion of a freestanding graphene membrane exhibits Brownian motion with rare large-height excursions indicative of Lévy walks. In addition, this motion was shown to follow a heavy-tailed Cauchy-Lorentz velocity probability distribution function (PDF),

$$p(v,\gamma) = \frac{\gamma}{\pi(\gamma^2 + v^2)}, \tag{4}$$

where γ is a constant, rather than the Maxwell-Boltzmann distribution[10]. Other results related to the anomalous dynamics of freestanding graphene membranes are described in [11–14]. This discovery is surprising, requiring a new perspective for understanding the properties of freestanding graphene membranes. In addition, it may be possible to take advantage of this special velocity distribution by converting the higher values of the kinetic energy of graphene membranes into electrical energy [15]. This noisy motion could represent a new renewable power source or physical battery [16–19] that provides clean energy.

A deeper theoretical understanding of the origin of this unusual velocity distribution is needed to realize its potential value. Molecular dynamic simulations point to ripple curvature inversion as a possible mechanism [10], but only one ripple is considered with clamped boundary conditions. A broader theoretical foundation is necessary to help uncover a deeper understanding of the anomalous dynamics of the freestanding graphene membrane. For example, one problem with the Cauchy-Lorentz distribution is that the expectation of the velocity square $E(v^2)$ is $+\infty$, which means that the average kinetic energy is $+\infty$. However, in accordance with the basic theory of statistical physics [20], the temperature is proportional to the average kinetic energy, namely, $T \propto E(v^2)(\bar{\varepsilon})$, which means that T tends to infinity, which is not true. For these reasons, we will use the truncated Cauchy-Lorentz distribution. The comparisons shown in this paper show that the truncated Cauchy-Lorentz distribution is a better fit to the experimental data when compared with both the Cauchy-Lorentz distribution and Maxwell-Boltzmann distribution.

2. Construction of Truncated Cauchy-Lorentz Distribution

In this section, three methods are applied to construct the truncated Cauchy-Lorentz distribution: the Fokker-Planck-Kolmogorov equation method, the maximum nonsymmetric entropy principle [21, 22], and the Bayesian inference by maximum entropy principle [23]. For each method, we first identify the necessary restrictions applied to the model; then obtain the desired probability distribution function (PDF).

2.1. The Fokker-Planck-Kolmogorov Equation Method. The traditional Langevin equation separates the impacts from the surrounding medium into two parts, as follows:

$$m\dot{x} = -\lambda\dot{x} + \xi(t), \tag{5}$$

where m is the mass of the carbon atom under consideration, the first term on the right hand side is the averaged-out viscous drag, and $\xi(t)$ represents the rapidly fluctuating random force, satisfying

$$\begin{aligned} \langle \xi(t) \rangle &= 0, \\ \left\langle \xi(t), \xi\left(t'\right) \right\rangle &= \delta\left(t - t'\right) \end{aligned} \tag{6}$$

where the symbol $\langle \ldots \rangle$ denotes ensemble averaging. The success of this method led to the development of the generalized Langevin equation, given by

$$m\dot{v} = f(v,t) + g(v,t)\,\xi(t), \tag{7}$$

where f, g are two functions. The general function f now represents the impact of the viscous drag from the medium. For our model, we set f to zero. Since the experiments on the freestanding graphene membrane are performed under vacuum, the effect of the neighboring bonded carbon atoms can be completely described using only the rapid fluctuation force. With this simplification, the modified Langevin equation becomes

$$m\dot{v} = g(v,t)\,\xi(t). \tag{8}$$

After taking the average of both sides and relating it to the Fokker-Planck-Kolmogorov master equation, we obtain the following equation [24]:

$$\frac{\partial p(v,t)}{\partial t} = \frac{1}{2}\frac{\partial^2 p(v,t)}{\partial^2 v}\left(g^2(v)\,p(v,t)\right), \tag{9}$$

where $p(v,t)$ is the PDF we are seeking. If we choose g to be

$$g(v) = \sqrt{v^2 + \gamma^2}, \tag{10}$$

where γ is a constant, then the PDF generated by (9) is the truncated Cauchy-Lorentz distribution, given by

$$p(v) = \frac{C}{\gamma^2 + v^2}, \tag{11}$$

where C is an integral constant used to ensure

$$\int_{-k}^{k} p(v)\,dv = 1, \tag{12}$$

where $(-k, k)$ is the velocity range of the distribution. In practice, the parameters C and γ in (10) are determined by numerical fitting, while k is fixed by the experimental results.

With the functional form of g determined, as shown in (10), insights may be gleaned about graphene's characteristics. As previously stated, the function g represents the strength of the rapidly fluctuating random force. This force is transmitted through the chemical bonds in the regular hexagonal structure of a graphene membrane (see Figure 1). When a neighboring carbon atom moves, the linked covalent bond transmits the effect of this movement to the carbon atom being modeled by Langevin's equation. This is the origin of the random force in (7). Moreover, given that (8) depends solely on the velocity, we can establish a relationship between the strength of the random force and the velocity.

Beginning with the kinetic theory of gases, we know that the frequency of collisions, ν, is proportional to the velocity and is given by the following expression:

$$\nu = n\pi a^2 v, \tag{13}$$

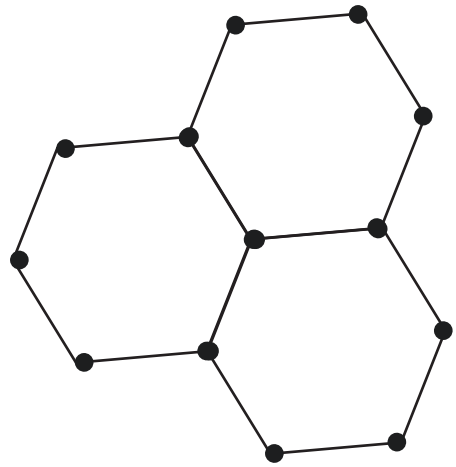

Figure 1: Schematic diagram of carbon atoms' structure in a graphene membrane.

where n is the number density, a is the distance between the particles, and v is the velocity. But, for the graphene lattice, the distance between two particles is the lattice constant. From this, we can rewrite (13) and obtain

$$a^2 = \frac{v}{n\pi v}. \tag{14}$$

Next, recall that the strength of the covalent bond is proportional to the inverse of the square of the distance, namely,

$$g \propto \frac{1}{a^2}. \tag{15}$$

After comparing (14)-(15), we find the desired relationship between the velocity of the carbon atom and the strength of the random force:

$$g \propto v^1. \tag{16}$$

Of course, there can be other factors which may influence the strength of the random force. From the experimental data, we know that the tunneling current and bias voltage impact the width of the PDF (see Figure 2 in [10]) and that the parameter γ in (10) will characterize these effects.

2.2. Maximum Nonsymmetric Entropy Principle. Next, we used the maximum nonsymmetric entropy principle proposed by Liu to construct the PDF [21, 22]. Using this method, a large number of important distribution laws can be easily and naturally derived, especially when compared to the traditional maximum entropy principle method. For example, the exponential and Gaussian distributions can be derived very easily. In addition, the nonsymmetric entropy approach is more expedient than other entropy approaches, such as the Tsallis's entropy, in deriving power law distributions. The key idea behind this method is to regard each event as providing some auxiliary information so that the total information of the event is defined by $I = -\ln p_j - \ln \beta_j$, where β_j is an auxiliary parameter of the jth event, and $\ln \beta_j$ is the auxiliary information. This method is equivalent to giving different weights to different particles in a system. In principle, by defining different functions for the nonsymmetric entropy, we can obtain different distribution laws. Moreover, in constructing the distribution, we learn what constraint must be imposed on the system. The starting point is the definition of the nonsymmetric entropy [21, 22], given by the following for discrete systems:

$$S(p_1, p_2, \ldots, p_n) = -\Sigma_{i=1}^{n} p_i \ln(\beta_i p_i), \tag{17}$$

or the following for continuous systems:

$$S(p) = -\int p(x) \ln[\beta(x)\, p(x)]\, dx, \tag{18}$$

where the right side of (18) is a definite integral, and the integration range is the domain of the random variable. Comparing these equations with the traditional symmetric entropy equations [25] given by the following for discrete systems

$$S(p_1, p_2, \ldots, p_n) = -\Sigma_{i=1}^{n} p_i \ln p_i, \tag{19}$$

or the following for continuous systems

$$S(p) = -\int p(x) \ln p(x)\, dx, \tag{20}$$

it is clear that the nonsymmetric method is equivalent to the symmetric method with different weights applied. Next, we imposed the condition that the entropy increases monotonically (per the second law of thermodynamics) and used differential calculus (discrete system (17)) or the variational method (continuous system (18)) to get the probability distribution function. In principle, if we choose the proper form for $\beta_i(\beta(x))$ and include the proper constraints, any desired distribution may be obtained. Given that this is a relatively new method, an illustration may be helpful. If we assume $\int x\rho(x) = \mu$, then we know

$$\rho(x) = \frac{1}{\beta(x)} \exp(a + bx), \tag{21}$$

where a and b are constants introduced to satisfy two constraints: $\int \rho(x) = 1$ and $\int x\rho(x) = \mu$. The power of this method is that by inspection we set

$$\beta(x) = \exp\left(\frac{x^2}{2}\right) \tag{22}$$

and obtain the Maxwell-Boltzmann PDF.

Next, we prove that there exists an auxiliary information parameter function $\beta(x)$, which maximizes the nonsymmetric entropy (18), and then choose this function to give us the truncated Cauchy-Lorentz PDF.

Proof. We will use the Lagrangian multiplier method within the variational method. First, we construct the following auxiliary functional:

$$\begin{aligned} S(p) = &-\int p(x)\ln\beta(x)\,p(x)\,dx \\ &+\lambda_1\left(\int p(x)\,dx - 1\right), \end{aligned} \tag{23}$$

where λ_1 is a constant. Then, according to the variational method, $S(p)$ reaches the maximum value corresponding to the condition of $\delta S/\delta p = 0$, which yields

$$\delta S = \left(\lambda_1 - \ln\beta(x)\,p(x) - 1\right)\delta p. \tag{24}$$

It follows that

$$\beta(x) = \frac{\exp(1-\lambda_1)}{p(x)}. \tag{25}$$

This shows that the PDF and the auxiliary function are simply related. By inspection, we set

$$\beta(x) = x^2 + \gamma^2, \tag{26}$$

$$\exp(1-\lambda_1) = C. \tag{27}$$

By replacing x with v, we can obtain the desired truncated Cauchy-Lorentz distribution (4). □

As previously mentioned, the auxiliary information parameter function β represents the weights assigned to different carbon atoms. So, (26) tells us that the higher the speed of the carbon atom is, the smaller the probability that this will occur. Alternatively, the majority of the particles have a velocity near zero, which is our expectation for any random process. In addition, the probability decreases as the speed increases, but in a manner that is relatively slow compared to the Maxwell-Boltzmann PDF. This gives the carbon atoms in freestanding graphene a heavy-tailed distribution, consistent with experimental findings.

Remark. There may be additional insights to be gained about the inner structure of the freestanding graphene membrane (from the constraints and auxiliary information parameter function β yielding the truncated Cauchy-Lorentz distribution), but for this study we show only the simplest situation. Other conditions will be explored in future work.

3. Bayesian Inference by Maximum Entropy Principle

Parameter estimation is an important aspect of statistics [26]. Bayesian inference [23, 27] is a useful tool in dealing with this problem. By regarding the probability distribution of random variable X as a random variable, then (according to the distribution of the parameters and the maximum entropy principle) the constraints that maximize the entropy may be found. This yields the PDF. In the discrete case, the differential equations must be solved, while in the continuous case, the variational equations must be solved.

In order to get the truncated Cauchy-Lorentz distribution by the Lagrangian multiplier method, the entropy is defined as

$$\begin{aligned} S(p) = &-\int p(v)\ln p(v)\,dx + \lambda_1\left(\int p(v) - 1\right) \\ &+\lambda_2 G(p). \end{aligned} \tag{28}$$

Then, according to the variation method and the maximum entropy principle,

$$\frac{\delta S}{\delta p} = -(1+\ln p) + \lambda_1 + \lambda_2\frac{\delta G}{\delta p} = 0, \tag{29}$$

which yields

$$\frac{\delta G}{\delta p} = \frac{1-\lambda_1+\ln p}{\lambda_2}. \tag{30}$$

Substitute (4) into (30), with the result that

$$\frac{\delta G}{\delta p} = \frac{1-\lambda_1+\ln C}{\lambda_2} - \frac{\ln\left(v^2+\gamma^2\right)}{\lambda_2}. \tag{31}$$

Thus,

$$G = \frac{1-\lambda_1+\ln C}{\lambda_2} - \int\frac{\ln\left(v^2+\gamma^2\right)}{\lambda_2}p(v)\,dx, \tag{32}$$

and the constraint can be written as

$$E\left[\ln\left(v^2+\gamma^2\right)\right] = 1-\lambda_1+\ln C = const. \tag{33}$$

Namely, the expectation of the $\ln(v^2+\gamma^2)$ is a constant. Thus, by introducing this special constraint, the truncated Cauchy-Lorentz PDF may be determined.

Remark. From the procedure above, it is apparent that, under the constraint $E[\ln(v^2+\gamma^2)] = const$, the truncated Cauchy-Lorentz distribution can be directly obtained. We infer that this is related to the inner structure of the graphene; researching the details of this relationship will be the subject of future studies.

4. Results and Discussion

Experimental values for the velocity of freestanding graphene come from 8×10^6 out-of-plane, height-time data points

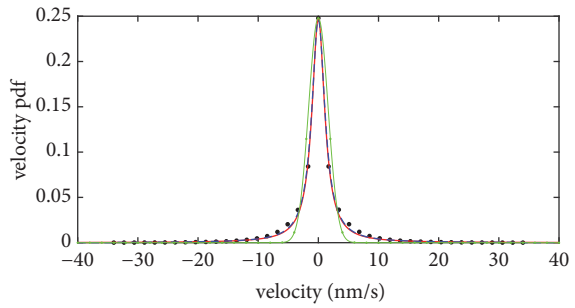

Figure 2: Velocity PDF: the solid line (red) represents the Cauchy-Lorentz distribution, the dashed line (blue) is the truncated Cauchy-Lorentz distribution, the "+" line (green) is the Gaussian distribution, and the black dots are the experimental data, when I=0.1 (tunneling current) and V=0.1 (bias voltage).

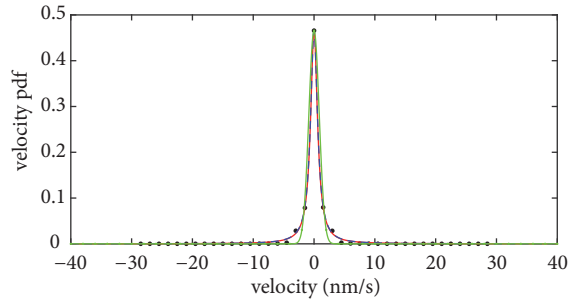

Figure 3: Velocity PDF: the solid line (red) represents the Cauchy-Lorentz distribution, the dash line (blue) is the truncated Cauchy-Lorentz distribution, the "+" line (green) is the Gaussian distribution, and the black dots are the experimental data, when I=0.01 (tunneling current) V=0.01 (bias voltage).

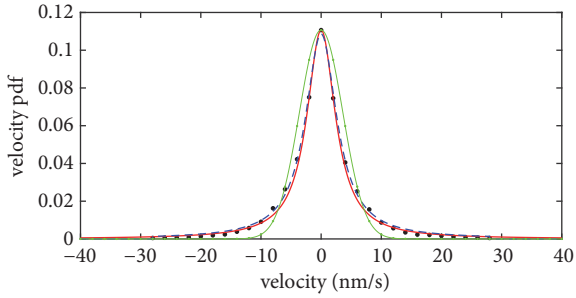

Figure 4: Velocity PDF: the solid line (red) represents the Cauchy-Lorentz distribution, the dashed line (blue) is the truncated Cauchy-Lorentz distribution, the "+" line (green) is the Gaussian distribution, and the black dots are the experimental data, when I=0.1 (tunneling current) and V=0.1 (bias voltage).

measured with a scanning tunneling microscope. This is feedback-on, constant current (0.1 nA), and constant voltage (0.1 V) data. Additional details are presented elsewhere (see [10]). From the velocity data, an experimental velocity PDF was created and plotted as blue circles in Figure 2. Overlaid on this data are three best-fit PDFs, including the truncated Cauchy-Lorentz, shown as a dashed blue line; the Cauchy-Lorentz, shown as a solid red line; and the Maxwell-Boltzmann, shown with green "+" signs. The PDFs are set to be equal to the data at zero speed. Note how well the truncated Cauchy-Lorentz PDF follows the data.

Additional experimental data acquired sequentially from one particular location on the freestanding graphene is shown in Figures 3, 4, and 5. The only experimental parameter varying between the measurements was the tunneling current setpoint: it went from 0.01 nA to 0.1 nA, then to 10.0 nA. As the tunneling current increases, the width of the velocity PDF increases. This is consistent with current-induced sample heating. For each figure, the same three best-fit velocity PDFs are displayed using the same line types as described earlier. In all cases, the truncated Cauchy-Lorentz PDF captures the unusually high velocities occurring with an exceptionally high probability. The other two distributions fall off too quickly, failing to capture the heavy-tailed property as well as the truncated Cauchy-Lorentz PDF does. The heavy-tailed part of the distribution is the key aspect for potential applications.

To quantify the quality of fit, three measures are presented: goodness of fit, variance, and mean variation. The results are summarized in Table 1, where it is clear that

Table 1: Three indexes of the distributions in different conditions of tunneling current and bias voltage, where T represents truncated Cauchy-Lorentz distribution, C means Cauchy distribution, and G is the Gaussian distribution.

	goodness of fit (T, C, G)	variance (T, C, G)$\times 10^4$	mean variation (T, C, G)
I=0.1, v=0.1	(0.9964, 0.9969, 0.9152)	(0.0639, 0.0541, 1.9580)	(0.0099, 0.0102, 0.0077)
I=0.01, v=0.01	(0.9985, 0.9986, 0.9892)	(0.0811, 0.0757, 0.6265)	(0.0092, 0.0093, 0.0084)
I=0.1, v=0.01	(0.9969, 0.9943, 0.9418)	(0.0223, 0.0392, 0.6118)	(0.0013, 0.0013, 0.0049)
I=10, v=0.01	(0.9989, 0.9199, 0.9585)	(0.0016, 0.1192, 0.0875)	(0.0003, 0.0031, 0.0026)

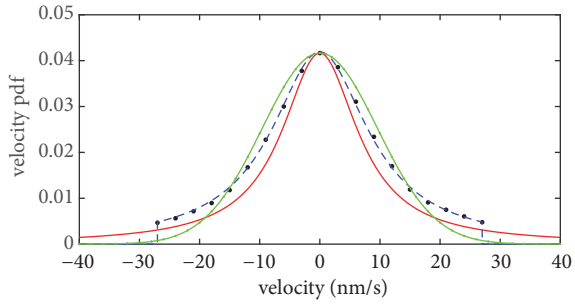

Figure 5: Velocity PDF: the solid line (red) represents the Cauchy-Lorentz distribution, the dashed line (blue) is the truncated Cauchy-Lorentz distribution, the "+" line (green) is the Gaussian distribution, and the black dots are the experimental data, when I=0.1 (tunneling current) and V=10 (bias voltage).

the truncated Cauchy-Lorentz distribution is superior to the other two.

Determining that graphene is continuously moving, even with a bias voltage applied, and that this motion is characterized by a non-Gaussian velocity distribution is a significant finding. Landmark theory papers published in the 1990s showed that the transportation of particles can be induced from this type of nonequilibrium fluctuation [28, 29]. In fact, a particular simulation for a freestanding graphene nanoribbon shows its energy harvesting opportunity [30].

Nonlinear processes with a non-Gaussian character have been increasingly observed in recent studies; therefore, an efficient model describing such dynamics is needed. In this paper, we have investigated the anomalous dynamic behavior of carbon atoms in a freestanding graphene membrane from three different perspectives, including the Fokker-Planck-Kolmogorov equation, the maximum nonsymmetric entropy principle, and the Bayesian inference by maximum entropy principle. For the generalized Langevin equation, we first modified the equation based on our understanding of physical properties of graphene in a vacuum. This allowed us to ignore the viscous force but maintain the important long jumps responsible for Lévy walks, which in turn gives us the heavy tails in the velocity PDF. Next, by combining collision theory with the lattice constraint, we showed that the random force is linear in the velocity. We handle finite temperature effects, such as current-induced heating, by truncating the Cauchy-Lorentz distribution. The accuracy of the fits indicates that the modified Langevin equation presented in the paper is reasonable. Moreover, the two methods of estimation helped us to learn more about the internal properties of freestanding graphene by the constraints they impose. Although the constraint used in each method is not unique, and only the most basic situation is presented, the dynamics of the inner structure of a graphene membrane can be inferred. Furthermore, the analytical nature of the perspective described in this paper sheds light on the origin of the anomalous dynamics of the heavy-tailed distribution.

Finally, we conclude that the three methods applied are useful for explaining certain nonlinear features of the anomalous dynamics of carbon atoms in freestanding graphene membranes, as well as for other physical processes. In addition, through [8], we can link our anomalous kinetics with chaotic dynamics. A direct numerical comparison between the findings of this paper and a chaotic dynamical system, with the aim of studying anomalous transport properties, is a promising topic for future research. With the insights obtained from this study, we hope to better understand and quantify the fundamental mechanisms of energy harvesting.

Data Availability

The date used to support the findings of this study are available from the corresponding author upon request.

Conflicts of Interest

We would like to declare that there are no conflicts of interest.

Acknowledgments

This work is supported by the Natural Science Foundation of China under Grant no. 11872280, Office of Naval Research under Grant no. N00014-10-1-0181, and the National Science Foundation under Grant no. DMR-0855358.

References

[1] R. Brown, "XXVII. *A brief account of microscopical observations made in the months of June, July and August* 1827, *on the particles contained in the pollen of plants; and on the general existence of active molecules in organic and inorganic bodies*," *Philosophical Magazine*, vol. 1828, 4, no. 21, pp. 161–173, 2009.

[2] R. Brown, "XXIV. *Additional remarks on active molecules*," *Philosophical Magazine*, vol. 1829, 6, no. 33, pp. 161–166, 2009.

[3] A. Einstein, "On the motion of small particles suspended in liquids at rest required by the molecular-kinetic theory of heat," *Annalen der Physik*, vol. 17, pp. 549–560, 1905.

[4] J. Millis, "Brownian movements and molecular reality," *Science*, vol. 33, no. 846, pp. 426-427, 1911.

[5] P. Langevin, "On the theory of brownian motion," *CR Acad Sci*, vol. 146, pp. 530–533, 1908.

[6] R. Kubo, "The fluctuation-dissipation theorem," *Reports on Progress in Physics*, vol. 29, no. 1, article no. 306, pp. 255–284, 1966.

[7] P. Lévy and M. É. Borel, *Théorie De Laddition Des Variables Aléatoires*, Gauthier-Villars, Paris, 1954.

[8] M. F. Shlesinger, G. M. Zaslavsky, and J. Klafter, "Strange kinetics," *Nature*, vol. 363, no. 6424, pp. 31–37, 1993.

[9] E. W. Montroll and M. F. Shlesinger, "Maximum entropy formalism, fractals, scaling phenomena, and 1/f noise: a tale of tails," *Journal of Statistical Physics*, vol. 32, no. 2, pp. 209–230, 1983.

[10] M. Ackerman, P. Kumar, M. Neek-Amal, P. Thibado, F. Peeters, and S. Singh, "Anomalous dynamical behavior of freestanding graphene membranes," *Physical Review Letters*, vol. 117, no. 12, Article ID 126801, 2016.

[11] P. Xu, Y. Yang, S. D. Barber et al., "Atomic control of strain in freestanding graphene," *Physical Review B: Condensed Matter and Materials Physics*, vol. 85, no. 12, pp. 1311–1318, 2012.

[12] M. Neek-Amal, P. Xu, J. Schoelz et al., "Thermal mirror buckling in freestanding graphene locally controlled by scanning tunnelling microscopy," *Nature Communications*, vol. 5, no. 1, article 4962, 2014.

[13] P. Xu, M. Neek-Amal, S. D. Barber et al., "Unusual ultra-low-frequency fluctuations in freestanding graphene," *Nature Communications*, vol. 5, no. 4, article no. 3720, 2014.

[14] J. K. Schoelz, P. Xu, V. Meunier et al., "Graphene ripples as a realization of a two-dimensional ising model: a scanning tunneling microscope study," *Physical Review B: Condensed Matter and Materials Physics*, vol. 91, no. 4, Article ID 045413, 2015.

[15] C. Shumaker, *Using the Natural Motion of 2D Materials to Create a New Source of Clean Energy*, 2017, https://researchfrontiers.uark.edu/good-vibrations/.

[16] E. Menya, P. W. Olupot, H. Storz, M. Lubwama, and Y. Kiros, "Production and performance of activated carbon from rice husks for removal of natural organic matter from water: a review," *Chemical Engineering Research and Design*, vol. 129, pp. 271–296, 2018.

[17] M. Gharabaghi, M. Irannajad, and A. R. Azadmehr, "Leaching kinetics of nickel extraction from hazardous waste by sulphuric acid and optimization dissolution conditions," *Chemical Engineering Research and Design*, vol. 91, no. 2, pp. 325–331, 2013.

[18] J. P. Vanden Heuvel, B. I. Kuslikis, and R. E. Peterson, "Covalent binding of perfluorinated fatty acids to proteins in the plasma, liver and testes of rats," *Chemico-Biological Interactions*, vol. 82, no. 3, pp. 317–328, 1992.

[19] M. Krachler, R. Alvarez-Sarandes, and G. Rasmussen, "High-resolution inductively coupled plasma optical emission spectrometry for 234U/238Pu age dating of plutonium materials and comparison to sector field inductively coupled plasma mass spectrometry," *Analytical Chemistry*, vol. 88, no. 17, pp. 8862–8869, 2016.

[20] L. D. Landau and E. M. Lifshitz, *Statistical Physics*, Pergamon Press, Oxford, UK, 2nd edition, 1980.

[21] C.-S. Liu, "Maximal non-symmetric entropy leads naturally to Zipf's law," *Fractals*, vol. 16, no. 1, pp. 99–101, 2008.

[22] C.-s. Liu, "Nonsymmetric entropy and maximum nonsymmetric entropy principle," *Chaos, Solitons & Fractals*, vol. 40, no. 5, pp. 2469–2474, 2009.

[23] F. J. Anscombe, "Bayesian statistics," *Science*, vol. 149, no. 3686, p. 850, 1965.

[24] R. Mannella, "Numerical integration of stochastic differential equations," 1997, https://arxiv.org/abs/hep-ph/9709326.

[25] G. L. Salinger and F. W. Sears, *Thermodynamics, Kinetic Theory and Statistical Thermodynamics*, Addison-Wesley, Reading, Mass, USA, 1975.

[26] G. W. Snedecor, "Statistical methods," *Soil Science*, vol. 51, no. 2, p. 163, 1989.

[27] G. E. P. Box and G. C. Tiao, *Bayesian Inference in Statistical Analysis*, John Wiley & Sons, Hoboken, NJ, USA, 2011.

[28] M. O. Magnasco, "Forced thermal ratchets," *Physical Review Letters*, vol. 71, no. 10, pp. 1477–1481, 1993.

[29] C. R. Doering, W. Horsthemke, and J. Riordan, "Nonequilibrium fluctuation-induced transport," *Physical Review Letters*, vol. 72, no. 19, pp. 2984–2987, 1994.

[30] M. López-Suárez, R. Rurali, L. Gammaitoni, and G. Abadal, "Nanostructured graphene for energy harvesting," *Physical Review B: Condensed Matter and Materials Physics*, vol. 84, no. 16, pp. 2727–2730, 2011.